



Sorption characteristics of tetrabromobisphenol A by oxidized and ethylenediamine-functionalized multi-walled carbon nanotubes

Jun Zhang¹, Yunhai Zhang¹, Shuili Yu*, Yulin Tang

State Key Laboratory of Pollution Control and Resource Reuse, College of Environmental Science & Engineering, Tongji University, Shanghai 200092, China, Tel. +86 21 65982708; emails: zhangjungstone@163.com (J. Zhang), yunhaitj@hotmail.com (Y. Zhang), Tel./Fax: +86 21 65982708; emails: ysl@tongji.edu.cn (S. Yu), tangyulin@tongji.edu.cn (Y. Tang)

Received 18 December 2014; Accepted 14 August 2015

ABSTRACT

Two kinds of functional groups, carboxyl, and amidogen were attached to on multi-walled carbon nanotubes (MWCNTs) with mixed acid and ethylenediamine (EDA). Scanning electron microscopy and transmission electron microscopy characterization showed no distinguishable changes in morphology, but found defects on the walls of the modified MWCNTs, and X-ray diffraction characterization indicated that the MWCNTs still retain the graphite structure. The sorption kinetics, sorption isotherms, and thermodynamics of pristine and modified MWCNTs were also investigated. The results showed that the equilibrium sorption could be well modeled by a pseudo-second-order kinetic fit. The uptake of tetrabromobisphenol A (TBBPA) sharply decreased with increasing pH values under alkaline conditions and at higher temperatures. The sorption isotherms of TBBPA on MWCNTs were well described by Langmuir and Freundlich models. Carboxyl- and hydroxyl-functionalized MWCNTs (MWCNTs-O) have higher values of the change in the standard Gibbs free energy (ΔG°) than do the amino-functionalized MWCNTs (MWCNTs-N); this is in agreement with the phenomenon that MWCNTs-O have a slightly higher sorption capacity than MWCNTs-N. The calculated thermodynamic parameters suggest that the sorption of TBBPA onto the modified MWCNTs is a feasible, spontaneous, and exothermic process. It was also proposed that hydrophobic interactions and π - π interactions were dominant in TBBPA sorption onto MWCNTs. The three sorbents retain a high sorption capacity after five sorption and desorption cycles.

Keywords: Sorption; Kinetics; Thermodynamics; Tetrabromobisphenol A; Functionalized MWCNTs

1. Introduction

Brominated flame retardants (BFRs) have been widely used in industry and commerce for fire pre-

vention. Tetrabromobisphenol-A (TBBPA) is a cheap and common BFR, and accounts for around 60% of the total BFR market. In 2007, the production capacity of TBBPA in China was estimated to be 18,000 tons [1]. TBBPA and its derivatives can release into environment from various materials during the

*Corresponding author.

¹These two authors contributed equally to the preparation of this article and should be regarded as co-first authors.

manufacturing, recycling, and disposing processes [2]. They have been found in soil [3–6], dust [7], aquatic sediment [8], sewage sludge [9], wastewater [10], and source water [11–13]. Moreover, TBBPA has been detected in tissues of aquatic organisms, wildlife, and humans [14,15]. These findings are significant because it is reported that TBBPA could cause various possible toxic effects, such as immunotoxicity and neurotoxicity effects in mammals [16,17]; thus we are driven to find a feasible means of removal of this contamination.

Sorption technology is widely used in pollution control due to its effective reduction of organic or inorganic pollutants in the water without producing new harmful substances [18]; for these same reasons it is considered to be an effective method for TBBPA removal from aquatic environments [19,20]. In recent years, sorption materials containing carbon, such as active carbon, graphene [21,22], and carbon nanotubes (CNTs) [20] have become popular sorbents. CNTs are excellent sorbent materials due to their small size, large surface area, hollow-layered structures, and good chemical stability [18,20,23]. They have been proven have great potential as adsorbents for the removal of organic, inorganic, and biological pollutants [24–27]. Although CNTs provide for high sorption capacities, applying them to aqueous applications present some challenges since they are prone to dissolution and separation from aqueous solutions [28,29]. In order to improve the hydrophilicity of CNTs, organic or inorganic functional groups were grafted to the surface of the CNTs, which not only prevent agglomeration of CNTs but also increase the active sites for sorption [24,30–32]. Summarizing previous research, the modification and blending of CNTs with polymer and functional groups can be an effective method to overcome the dissolution problem.

In our current study, multiwall carbon nanotubes (MWCNTs) were treated by mixed acid in order to introduce carboxyl and hydroxyl functional groups onto the surfaces of MWCNTs (MWCNTs-O) and then amino-functionalized MWCNTs (MWCNTs-N) were prepared by reacting MWCNTs-O with EDA. The TBBPA removal efficiencies of pristine and modified MWCNTs were determined as a function of contact time, pH, initial TBBPA concentration, and temperature. The kinetics and thermodynamics of TBBPA sorption on MWCNTs-O and MWCNTs-N were also studied.

2. Materials and methods

2.1. Materials

Tetrabromobisphenol-A (4,4-isopropylidenebis(2,6-dibromophenol)) (purity > 97%) and methanol (HPLC

grade) were purchased from the Sigma–Aldrich Company (MO, USA). MWCNTs were from Seldon Technology (VT, USA) and had nominal outer diameters of 10–20 nm, inner diameters of 5–10 nm, and a purity of >97%. Ultra pure water was obtained directly from a Milli-Q Integral system (Millipore, MA, USA) with a resistivity as high as 18.2 MΩ cm. EDA and *n,n*-dicyclohexylcarbodiimide (DCC, 99%) were purchased from the Aladdin Company (Shanghai, China). The other chemicals and reagents used in this study were of analytical grade and purchased from Sinopharm Chemical Reagents (Shanghai, China).

2.2. Preparation of MWCNTs-O and MWCNTs-N

First, the raw MWCNTs were put into a mixture of concentrated sulfuric acid and nitric acid (v/v, 3/1) and the mixture was sonicated for 12 h at 313 K in an ultrasonic bath. The mixture was then refluxed and stirred in a concentrated H₂SO₄ and 30% hydrogen peroxide (v/v, 4/1) solution at 343 K for 24 h. Then the mixture was refluxed in concentrated HNO₃ at 393 K for 24 h. Finally, after natural cooling to room temperature, the material was washed with water and dried in a vacuum-freeze dryer. This process resulted in carboxyl- and hydroxyl-functionalized MWCNT samples referred to as MWCNTs-O.

MWCNTs-O were then weighed and added to an EDA solution. Then the mixture was stirred at 298 K, and excess DCC was added and refluxed for 48 h at 353 K. After treatment, the mixture was washed with ethanol and vacuum filtered by a PTFE membrane filter with a 0.45 μm pore size and dried in a vacuum-freeze dryer. This additional processing resulted in amino-functionalized MWCNT samples referred to as MWCNTs-N.

2.3. Characterization

The microstructure and morphology of the pristine and modified MWCNTs were investigated with the following characterization methods: scanning electron microscopy (SEM; Philips XL30, Netherlands), transmission electron microscopy (TEM; JEOL 2011, Japan), and X-ray diffraction (XRD; D8 Advance, Bruker, Germany). The pH values of the supernatants were measured with an S20 SevenEasy pH meter (Mettler-Toledo, Shanghai, China).

2.4. Analytical methods

Concentrations of TBBPA were measured through ultra-performance liquid chromatography (UPLC;

ACQUITY UPLC H-Class, Waters, MA, USA) equipped with a TUV detector and a reversed phase BEH C18 Column (2.1×50 mm, $1.7 \mu\text{m}$). The column was maintained at 303 K when the samples were analyzed and the detection wavelength was set to 209 nm. TBBPA was performed in an isocratic elution program with methanol/water used as the mobile phase (v/v, 75/25). The injection volume of TBBPA was $10 \mu\text{L}$ and flow rate was maintained at 0.2 mL/min during the analysis.

The TBBPA and TBBPA-loaded MWCNTs were characterized by a Fourier transform infrared (FTIR) spectra (Nicolet5700, America Spectrum One, Perkin Elmer, MA, USA) between $4,000$ and 500 cm^{-1} .

2.5. Batch sorption experiment

In order to evaluate the characteristics of TBBPA sorption onto the MWCNTs, batch experiments were employed. The initial concentration of TBBPA solution was approximately 2.0 mg/L . In order to maintain a stable ionic strength, a 0.01 M NaCl background solution was used. Then $200 \mu\text{L}$ of the MWCNT stock solution (10 mg/mL) was injected into the solution. The pH values were adjusted by adding 0.1 M HCl and 0.1 M NaOH solutions. Afterward, the flasks containing the solution were transferred to a thermostatic air shaker operating at 180 rpm . After the designated amount of time ($3, 6, 10, 15, 20, 30, 40, 60, 120, 360,$ and 720 min), 1.0 mL of the mixture solution was extracted and centrifuged at $12,000 \text{ rpm}$ for 5 min . The supernatants were then analyzed by UPLC to measure the residual concentrations of TBBPA. The reported sorption values are averages taken from the sorption experiments which were performed in triplicate. The TBBPA sorption on MWCNTs can be calculated by the following Eq. (1):

$$q_t = \frac{(C_0 - C_t)V}{m} \quad (1)$$

where q_e (mg/g) is the sorbed amount of TBBPA, C_0 and C_t (mg/L) are the concentration at initial time and time t (min), respectively, V (L) is the volume of solution, and m (g) is the mass of the MWCNTs in solution.

2.6. Desorption experiments

Desorption of TBBPA in the composites was carried out by washing the adsorbent with distilled water several times, followed by shaking the sorbents in ethanol at 180 rpm for 6 h in order to achieve complete desorption. The solid and liquid phases were

separated by vacuum filtration. The reusability of the composites was tested by evaluating their sorption performance for removal of TBBPA through five sorption/desorption cycles.

2.7. Sample preparation for FTIR analysis

A solution containing 10-mg MWCNTs and 250-mL TBBPA with a set concentration of 2 mg/L and pH 7.5 was transferred to conical flasks. Then, the mixed solution was shaken in a shaking table for 12 h under room temperature (25°C). Sorbents were separated by vacuum filtration equipment with a $0.45 \mu\text{m}$ ultrafiltration membrane. After vacuum filtration the sorbents were washed three times with deionized distilled water to remove any residual soluble TBBPA. Finally, the collected sorbents were vacuum dried for FTIR analysis.

3. Results and discussion

3.1. Physicochemical characterization of MWCNTs

A comparison of the SEM and TEM of the three types of MWCNTs are shown in Fig. 1. All samples maintained their original hollow tubular structure [33] and showed no distinguishable changes in morphology. However, defects were found on the walls of the modified MWCNTs, which is different than the pristine MWCNTs; these defects may indicate the location of the grafted functional groups. The XRD powder profiles of the pristine and modified MWCNTs are shown in Fig. 2. In these diffractograms, it is easy to find the characteristics of a typical MWCNT structure: with the typical peak of the (002)-graphite base plane at $2\theta = 25.8^\circ$ and the peak at approximately $2\theta = 42.8^\circ$ assigned to the (100)-graphite base plane [34]. These two characteristic peaks demonstrate that the CNTs still retain their graphite structure.

3.2. Effect of contact time on TBBPA sorption

The dynamics of TBBPA sorption onto the MWCNTs is shown in Fig. 3. The sorption process of TBBPA uptake for all three MWCNTs materials was quite rapid. The fastest sorption rate was found during the first 20 min with nearly 90% sorption capacity being consumed in that time. The maximum sorption capacity was achieved at approximately 30 min , and then the sorption capacity decreased slightly. The small drop in capacity from 60 to 120 min was mainly due to the large concentration gradient of pollutants between the solid-liquid phases, which produced a diffusion driving force to promote hydrophobic

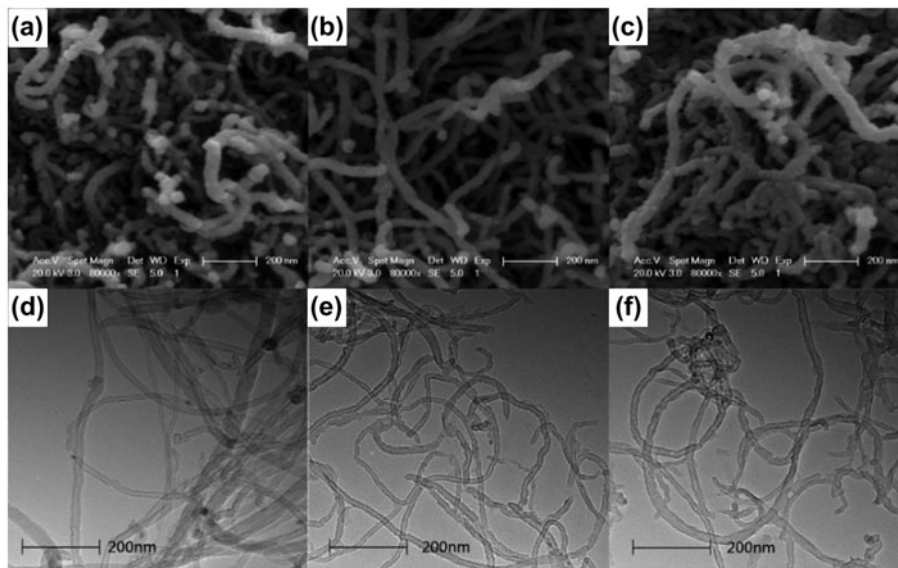


Fig. 1. SEM images of (a) pristine MWCNTs, (b) MWCNTs-O, and (c) MWCNTs-N; (d–f) are TEM images corresponding to the samples of (a–c), respectively.

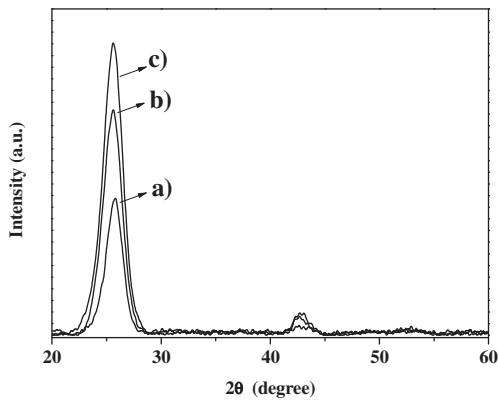


Fig. 2. XRD patterns of pristine MWCNTs (a), O-MWCNTs (b), and N-MWCNTs (c).

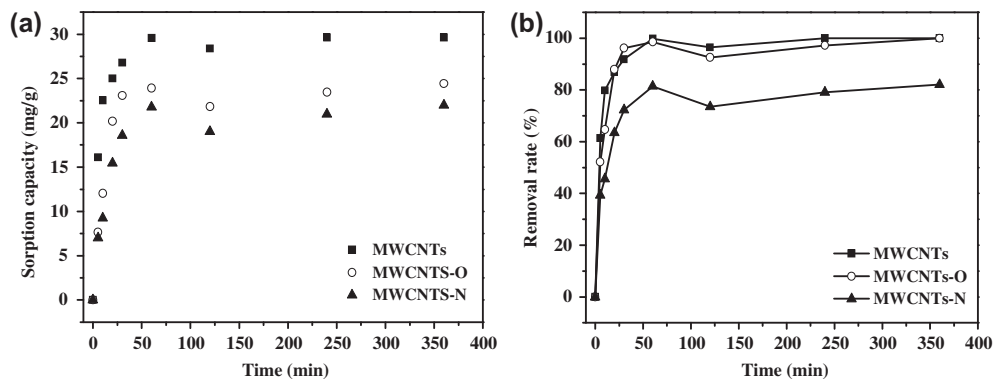


Fig. 3. The effect of contact time on (a) the TBBPA sorption capacity onto MWCNTs, MWCNTs and MWCNTs-N, and (b) the removal rate of TBBPA from solution.

organic compounds (HOC) moving quickly onto the sorbent surface [35]. As the sorption time increases, sorption was able to rebalance and the vast majority of TBBPA uptake was onto the active groups. Finally, the sorption reached dynamic equilibrium. After stabilization, it was found that the sorption capacity of the pristine MWCNTs had the largest sorption capacity (29.64 mg/g), while the MWCNTs-N had the smallest capacity (21.01 mg/g), and the sorption of MWCNTs-O was 22.92 mg/g.

3.3. Effect of pH value on TBBPA sorption

The sorption behavior was investigated at 303 K, while varying the pH values of the solution between 3.0, 4.0, 6.0, 7.0, 9.0, and 10.0 (± 0.3), respectively. The

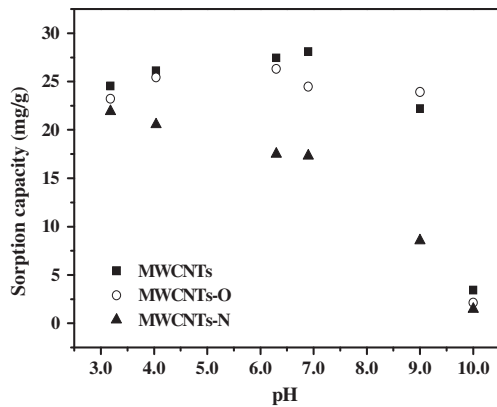


Fig. 4. The effect of pH on the TBBPA sorption capacity of pristine MWCNTs, MWCNTs-O, and MWCNTs-N.

effects of different pH values on TBBPA removal can be seen in Fig. 4. The uptake of TBBPA onto the pristine MWCNTs was maximized when pH 7.0. The sorption behavior of MWCNTs-O was similar to that of the pristine MWCNTs, but its maximum sorption capacity occurred when pH 6.0. The sorption of TBBPA onto MWCNTs-N decreased with increasing pH from 3.0 to 10.0. The amount of neutral molecular TBBPA decreased with increasing pH, and the sorption capacity decreased when the solution pH increased from 7.0 to 10.0, which is consistent with our previous studies [19,34]. When the $\text{pH} < \text{p}K_{a1}$, most of the TBBPA was in molecular form and more hydrophobic, which made it attach more easily to the MWCNTs. On the contrary, when the $\text{pH} > \text{p}K_{a1}$, the TBBPA increases in ionization and hydrophilicity; as a result, the sorption decreased, which may be due to the reduction of hydrophobic interactions [36,37]. As shown in Fig. 5 and our previous studies [34], the zeta

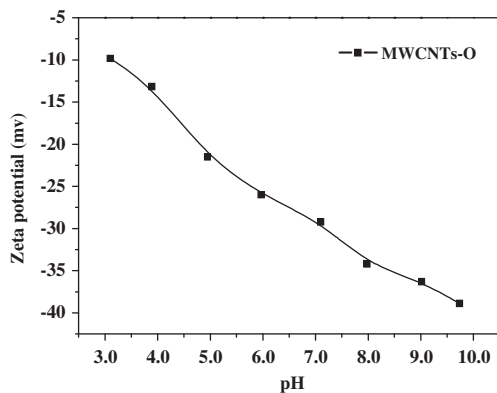


Fig. 5. Zeta potential of MWCNTs-O under various pH conditions.

potential of the three MWCNTs was negative and decreased as pH increased from 4.0 to 10.0. The MWCNTs-O had a lower zeta potential than the MWCNTs-N, while it owns a greater TBBPA sorption capacity. It can be inferred that the electrostatic repulsion between the negatively charged MWCNTs surface and the TBBPA anions may not act as the major driving force for sorption.

3.4. TBBPA sorption kinetics

The dynamics of TBBPA sorption onto MWCNTs is shown in Fig. 6. In order to find the rate of TBBPA sorption onto MWCNTs, pseudo-first-order and pseudo-second-order kinetic models were applied to investigate the sorption kinetics [38–42], which are expressed as Eqs. (2) and (3), respectively:

$$\log(q_e - q_t) = \log q_e - \frac{k_1 t}{2.303} \quad (2)$$

$$\frac{t}{q_t} = \frac{1}{k_2 q_e^2} + \frac{t}{q_e} \quad (3)$$

where k_1 (min^{-1}) and k_2 (g/mg min) are the pseudo-first and pseudo-second-order rate constants, respectively, and q_e (mg/g) and q_t (mg/g) are the equilibrium sorption capacity and sorption capacity at time t (min), respectively. The initial sorption rate h (mg/g h) can be determined from $h = k_2 q_e^2$.

The pseudo-first-order model did not fit the TBBPA sorption onto MWCNTs perfectly; this model worked for the first 60 min, but was unsuitable for the remainder of the sorption process. Additionally, the calculated equilibrium sorption capacities ($q_{e,\text{cal}}$) calculated by the pseudo-first-order model did not match the experimentally derived ($q_{e,\text{exp}}$) (as presented in Fig. 6(a) and Table 1). Zhang et al. also found that with the initial TBBPA concentration increasing to 1.0 mg/L, the reaction tended to be complex, and that it was difficult to use a specific model to simulate the TBBPA sorption onto graphene oxide (GO). However, it was approximated by the pseudo-second-order model to simulate the sorption process under experimental conditions [19]. As shown in Table 1, the $q_{e,\text{cal}}$ obtained from the pseudo-second-order model were very close to the $q_{e,\text{exp}}$. The pseudo-second-order model assumed that the sorption rate was controlled by chemical interaction and that the sorption capacity was proportional to the number of active sites on the sorbents [43]. It can be concluded that the rate of TBBPA uptake onto the MWCNTs is highly correlated with the number of active sites on the MWCNTs.

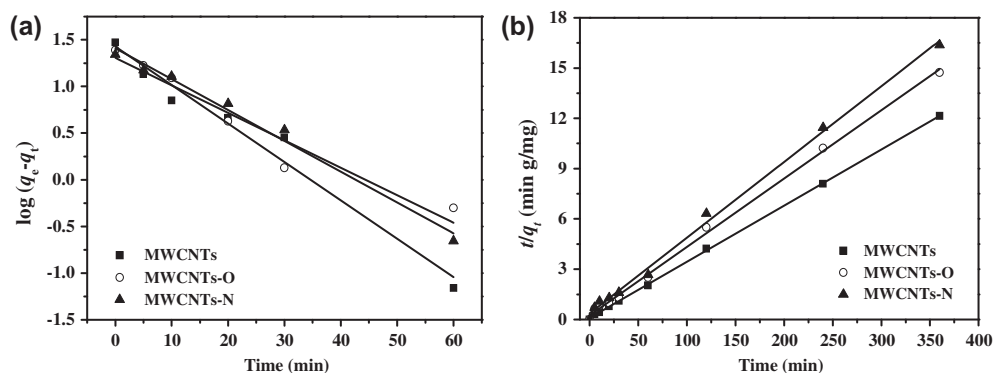


Fig. 6. The (a) pseudo-first-order kinetic and (b) pseudo-second-order kinetic plots for TBBPA sorption on pristine MWCNTs, MWCNTs-O, and MWCNTs-N.

Table 1

Kinetic parameters for TBBPA sorption on pristine MWCNTs, MWCNTs-O, and MWCNTs-N

Sorbents	Pseudo-first-order kinetic model				Pseudo-second-order kinetic model			
	$q_{e,exp}$ (mg/g)	$q_{e,cal}$ (mg/g)	k_1 (min ⁻¹)	R^2	$q_{e,cal}$ (mg/g)	k_2 (min ⁻¹)	h (mg/g min)	R^2
MWCNTs	30.13	26.69	0.0949	0.9709	29.86	0.0114	10.1	0.9997
MWCNTs-O	22.92	20.28	0.0679	0.9388	24.52	0.0066	3.96	0.9978
MWCNTs-N	21.01	25.63	0.0762	0.9871	22.17	0.0053	2.60	0.9972

3.5. Effect of solution temperature on TBBPA removal

Generally, the solution temperature is an important factor affecting sorption. The effect of temperature on the behavior of TBBPA sorption onto MWCNTs was analyzed by conducting sorption experiments under various temperatures from 283 to 313 K. Investigation of pristine MWCNTs has been done in previous reports [29,31], therefore, only the two modified MWCNTs were studied in this work.

In our study, two classical equilibrium isotherm models were applied to describe the experimental data, namely the Langmuir and Freundlich isotherm models. The Langmuir sorption model assumes that maximum sorption corresponds to a saturated monolayer of the molecules on the adsorbent surface, with no lateral interaction between the sorbed molecules. The linear equation for Langmuir isotherm is:

$$\frac{C_e}{q_e} = \frac{C_e}{q_{max}} + \frac{1}{q_{max}b} \quad (4)$$

where q_{max} (mg/g) is the theoretical maximum sorption amounts, and b is the Langmuir model constant.

The Freundlich isotherm model is an empirical equation and used to describe heterogeneous surfaces [44]. The linear equation for Freundlich isotherm is:

$$\log q_e = \frac{\log C_e}{n} + \log K_F \quad (5)$$

where n and K_F are the Freundlich model constants.

The results of fitting the two models are shown in Fig. 7, and their fitting parameters are listed in Table 2. The regression correlation coefficients (R^2) exceed 0.95 for all fitting curves, suggesting that experimental data of both materials were well fit by both models. As shown in Table 2, the values of b and K_F decrease with increasing temperature, indicating that the TBBPA sorption capacity on MWCNTs-O and MWCNTs-N decreased with the increase in temperature. When n values lie between 1 and 10, the sorption process is energetically favorable. In our research, the values of n were 2.18, 2.56, 2.12 for MWCNTs-O and 1.77, 1.87, 1.91 for MWCNTs-N at 283, 298, and 313 K, respectively, illustrating that the batch sorption is favorable for all of the experimental conditions that were tried. Since the data for the sorption of TBBPA on MWCNTs-O and MWCNTs-N are well fit by the Langmuir model, it is an indication that the sorption process is monolayer sorption. Meanwhile, the calculated sorption capacity of MWCNTs-O was larger than that of MWCNTs-N at each temperature, which might indicate that the hydrophobicity of MWCNTs-O was

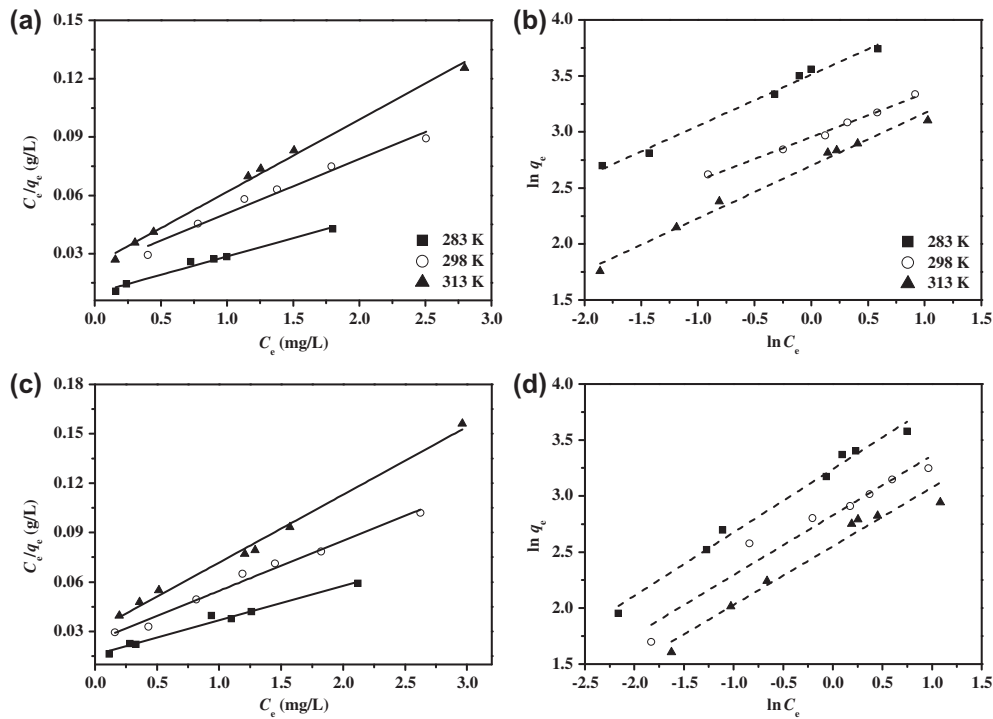


Fig. 7. The isotherms at different temperatures of TBBPA sorption by MWCNTs-O as compared to the (a) Langmuir and (b) Freundlich models and by MWCNTs-N as also compared to the (c) Langmuir and (d) Freundlich models.

Table 2
Isotherm parameters for TBBPA sorption on MWCNTs-O and MWCNTs-N

Sorbents	T (K)	Langmuir			Freundlich		
		q_m (mg/g)	b (L/mg)	R^2	K_F	n	R^2
MWCNTs-O	283	53.02	1.95	0.978	33.45	2.18	0.987
	298	35.79	1.23	0.968	19.18	2.56	0.991
	313	26.88	1.51	0.995	14.87	2.12	0.985
MWCNTs-N	283	47.87	1.31	0.983	25.57	1.77	0.987
	298	32.89	1.25	0.986	16.92	1.87	0.952
	313	24.27	1.35	0.993	12.83	1.91	0.958

greater than MWCNTs-N under current experimental conditions.

Table 2 shows that the maximum sorption capacities are determined to be 53.02 mg/g for MWCNTs-O and 47.87 mg/g for MWCNTs-N at 288 K. The uptake of TBBPA onto both materials was found to decrease as the solution temperature increased from 288 to 313 K. The sorption capacity of MWCNTs-O was greater than that of the MWCNTs-N at each temperature. Fasfous et al. [36] found that the sorption of TBBPA on pristine MWCNTs is exothermic and spontaneous at the temperatures they studied. Our

test results indicated that TBBPA uptakes on the modified MWCNTs were also an exothermic process.

3.6. Sorption thermodynamic analysis

The thermodynamic parameters can help us to understand the inherent energetic changes involved during the sorption process. In order to discuss the thermodynamic parameters, the sorption isotherms of TBBPA on modified MWCNTs were studied at 283, 298, and 313 K. Changes of the thermodynamic parameters for the standard free energy change of

sorption (ΔG° , kJ/mol), standard enthalpy change (ΔH° , kJ/mol), and standard entropy change (ΔS° , J/mol K) were calculated while varying the thermodynamic equilibrium constant, K_d , at the above temperatures.

For the sorption reaction, K_d can be calculated as follows:

$$K_d = \frac{q_e}{C_e} \quad (6)$$

It is possible to calculate K_d by plotting $\ln(q_e/C_e)$ vs. q_e . The data may then be fit by a straight line (as presented in Fig. 8) by linear curve fitting and the intercept of the vertical axis is the value of $\ln K_d$.

The changes in free energy for any interaction can be calculated by the following two equations:

$$\Delta G^\circ = -RT \ln K_d \quad (7)$$

$$\Delta G^\circ = \Delta H^\circ - T\Delta S^\circ \quad (8)$$

By rearranging Eqs. (7) and (8), it is possible to get a linear equation that may be used to calculate the values of ΔH° , ΔS° and ΔG° :

$$\ln K_d = -\frac{\Delta H^\circ}{RT} + \frac{\Delta S^\circ}{R} \quad (9)$$

where R is the universal gas constant (8.3145 J/mol K) and T is the sorption experiment temperature (K). By plotting $\ln K_d$ vs. $(1,000/T)$, the linear plot shown in Fig. 9 is obtained. Thermodynamic parameters ΔH° and ΔS° were separately found from the slope ($-\Delta H^\circ/R$) and the y -intercept ($-\Delta S^\circ/R$) and then the ΔG° was calculated with Eq. (9). The calculated thermodynamic parameters are shown in Table 3.

The values of ΔG° were negative at all temperatures, indicating that the sorption of TBBPA onto both MWCNTs-O and MWCNTs-N was a spontaneous and thermodynamically favorable process, and the randomness of the sorption system decreased with TBBPA uptake onto the two types of modified MWCNTs. Meanwhile, both the slight increase in ΔG° values from 288 to 313 K and the negative ΔH° values suggest that TBBPA uptake onto MWCNTs-O and MWCNTs-N is an exothermic process. This was further proven by the observation that the sorption of TBBPA onto modified MWCNTs decreased with increasing sorption temperature. It is generally understood that physical and chemical sorption involve an enthalpy change between 2–21 kJ/mol and 80–200 kJ/mol, respectively [45]. In our research, the ΔH° values were -23.01 kJ/mol for MWCNTs-O and -17.28 kJ/mol for MWCNTs-N, which suggests that the sorption of TBBPA on the two types of modified MWCNTs was mainly a physical sorption process.

3.7. Reusability of MWCNTs

The reusability of the MWCNTs, MWCNTs-O, and MWCNTs-N for TBBPA sorption was also evaluated (as shown in Fig. 10). The result indicated that the sorbents consistently exhibited good sorption capacity on TBBPA with the sorption capacity were observed 97, 92, and 95% of their initial values respectively even after five repeated sorption and desorption cycles, suggesting the three sorbents remained with good efficiency.

3.8. Sorption mechanism

Previous research has already reported that the π - π interaction was considered as one of the predominant driving forces for sorption of organic pollutants with a

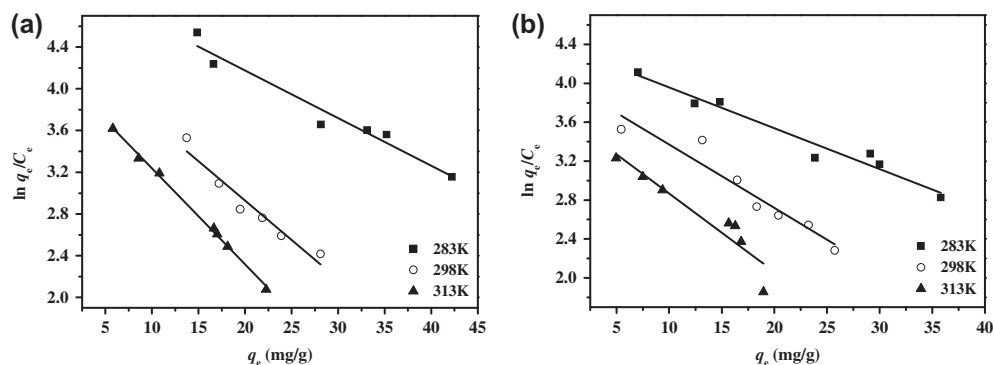


Fig. 8. Plot of $\ln(q_e/C_e)$ vs. q_e of TBBPA sorption on (a) MWCNTs-O and (b) MWCNTs-N at different temperatures.

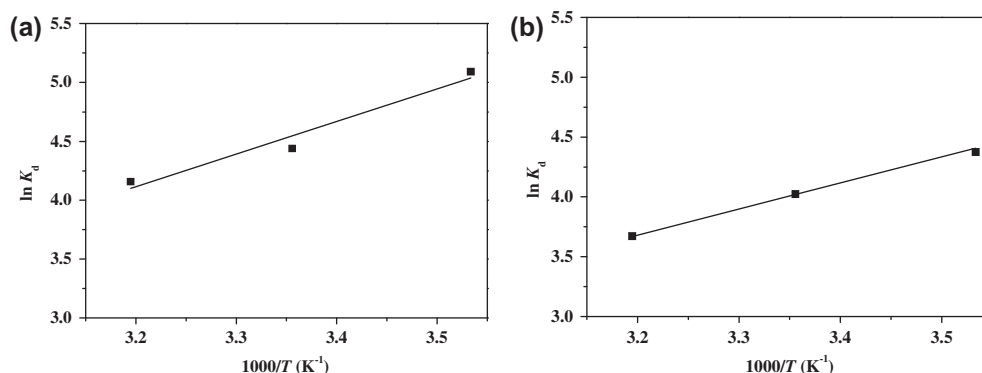


Fig. 9. Plot of $\ln(K_d)$ vs. $1000/T$ of TBBPA sorption onto (a) MWCNTs-O and (b) MWCNTs-N.

Table 3
Thermodynamic parameters of TBBPA sorption on MWCNTs-O and MWCNTs-N

	MWCNT-O			MWCNT-N		
	283 K	298 K	313 K	283 K	298 K	313 K
ΔG° (kJ/mol)	-11.85	-11.26	-10.59	-20.62	-9.94	-9.57
ΔS° (J/mol K)		-39.44			-24.62	
ΔH° (kJ/mol)		-23.01			-17.28	

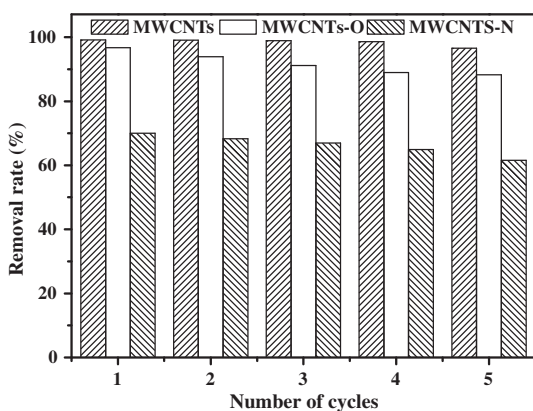


Fig. 10. The reusability of the CNTs, MWCNTs-O, and MWCNTs-N for TBBPA.

carbon-carbon double bond (C=C) or benzene rings on MWCNTs [25,46–48]. In order to investigate the possible mechanisms of the sorption of TBBPA on the three sorbents, the FTIR spectra of TBBPA, MWCNTs, MWCNTs-O, MWCNTs-N, and TBBPA loaded the three sorbents and were compared. As shown in Fig. 11, the intense peak around 3400 cm^{-1} can be attributed to the stretching vibration of the O–H groups. The peak around 1729 cm^{-1} was associated with the appearance of C=O bonds in carboxylic acid

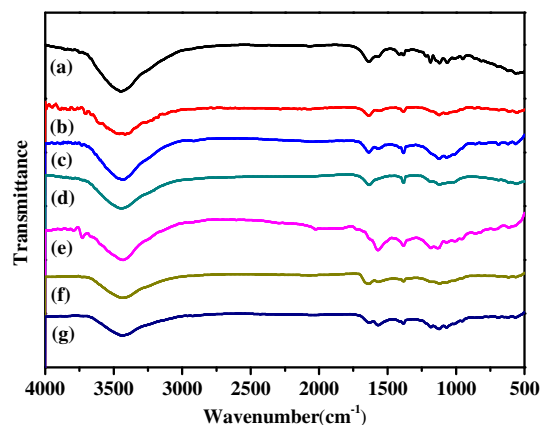


Fig. 11. FTIR spectra of (a) TBBPA, (b) MWCNTs, (c) TBBPA-loaded MWCNTs, (d) MWCNTs-O, (e) TBBPA-loaded MWCNTs-O, (f) MWCNTs-N, and (g) TBBPA-loaded MWCNTs-N.

and carbonyl moieties. The peak at 1560 cm^{-1} referred to the skeletal vibration of aromatic C=C bonds. The peak at around 1392 cm^{-1} was assigned to the carboxyl (O=C–O) bonds. The peak around 1220 cm^{-1} belonged to the epoxy (C–O–C) bonds [49,50]. Compared to the original sorbents, there were some new peaks at $900\text{--}1250\text{ cm}^{-1}$, which appeared or were strengthened in the FTIR spectrum of TBBPA loaded on the three

sorbents. These peaks were in accordance with the peaks from the FTIR spectrum of TBBPA, which demonstrated that a number of TBBPA molecules had been sorbed on the three sorbents. As shown in Fig. 11, the peaks of C=C stretching became smaller after the sorption process, while the peaks of O–H stretching almost unchanged, meaning that the π - π interaction strength was a main force for TBBPA loading on the three sorbents. What is more, the peaks of C=C stretching was decreased by the sequences in MWCNTs, MWCNTs-O, MWCNTs-N, which gave a possible explain to the phenomenon that the sorption capacity of TBBPA on the three sorbents obeys the following order: MWCNTs > MWCNTs-O > MWCNTs-N.

4. Conclusions

The sorption parameters of pristine and modified MWCNTs are evaluated for the removal of TBBPA. The sorption capacity increased with the increase in contact time, and decreased with increasing temperature for all three forms of the MWCNTs. The fastest removal rate was observed during the first 20 min with 90% of total sorption and the maximum sorption occurring at approximately 30 min. The behavior of pristine and modified MWCNTs at different pH values was mainly determined by the changes of hydrophobicity and solubility of TBBPA. Sorption of TBBPA on the three materials fit well with the pseudo-second-order kinetic model. The ΔG° value of the MWCNTs-O was higher than that of the MWCNTs-N, indicating that TPPBA was more easily sorbed onto the MWCNTs-O. The sorption of TBBPA on the modified MWCNTs was shown to be a thermodynamically feasible and spontaneous process. The ΔH° value suggested that the sorption is an exothermic and a physical sorption process. It was considered that the TBBPA could be sorbed on MWCNTs by hydrophobic interactions and π - π interactions. Additionally, all the three sorbents showed excellent stability of sorption capacity.

Acknowledgments

This work was supported by Key Projects in the National Science and Technology Pillar Program during the Twelfth Five-year Plan Period (2012BAJ25B06), Twelfth Five-year Plan Period of Major Science and Technology Program for Water Pollution Control and Treatment (2012ZX07403-001) and the Collaborative Innovation Center of Advanced Technology and Equipment for Water Pollution Control and the Collaborative Innovation Center for Regional Environmental Quality.

References

- [1] Z.X. Shi, Y. Jiao, Y. Hu, Z.W. Sun, X.Q. Zhou, J.F. Feng, J.G. Li, Y.N. Wu, Levels of tetrabromobisphenol A, hexabromocyclododecanes and polybrominated diphenyl ethers in human milk from the general population in Beijing, China, *Sci. Total Environ.* 452–453 (2013) 10–18.
- [2] M.S.E. Mäkinen, M.R.A. Mäkinen, J.T.B. Koistinen, A.L. Pasanen, P.O. Pasanen, P.I. Kalliokoski, A.M. Korpi, Respiratory and dermal exposure to organophosphorus flame retardants and tetrabromobisphenol A at five work environments, *Environ. Sci. Technol.* 43 (2009) 941–947.
- [3] W. Han, L. Luo, S.Z. Zhang, Adsorption of tetrabromobisphenol A on soils: Contribution of soil components and influence of soil properties, *Colloids Surf., A: Physicochem. Eng. Aspects* 428 (2013) 60–64.
- [4] D.Y. Huang, H.Q. Zhao, C.P. Liu, C.X. Sun, Characteristics, sources, and transport of tetrabromobisphenol A and bisphenol A in soils from a typical e-waste recycling area in South China, *Environ. Sci. Pollut. Res.* 21 (2014) 5818–5826.
- [5] S. Arnon, Z. Ronen, A. Yakirevich, E. Adar, Evaluation of soil flushing potential for clean-up of desert soil contaminated by industrial wastewater, *Chemosphere* 62 (2006) 17–25.
- [6] Y.N. Li, Q.X. Zhou, Y.Y. Wang, X.J. Xie, Fate of tetrabromobisphenol A and hexabromocyclododecane brominated flame retardants in soil and uptake by plants, *Chemosphere* 82 (2011) 204–209.
- [7] G. Di Napoli-Davis, J.E. Owens, Quantitation of tetrabromobisphenol-A from dust sampled on consumer electronics by dispersed liquid-liquid microextraction, *Environ. Pollut.* 180 (2013) 274–280.
- [8] M.J. He, X.J. Luo, L.H. Yu, J.P. Wu, S.J. Chen, B.X. Mai, Diastereoisomer and enantiomer-specific profiles of hexabromocyclododecane and tetrabromobisphenol A in an aquatic environment in a highly industrialized area, South China: Vertical profile, phase partition, and bioaccumulation, *Environ. Pollut.* 179 (2013) 105–110.
- [9] Z.H. Sun, L. Mao, Q.M. Xian, Y.J. Yu, H. Li, H.X. Yu, Effects of dissolved organic matter from sewage sludge on sorption of tetrabromobisphenol A by soils, *J. Environ. Sci. China* 20 (2008) 1075–1081.
- [10] I.K. Hwang, H.H. Kang, I.S. Lee, J.E. Oh, Assessment of characteristic distribution of PCDD/Fs and BFRs in sludge generated at municipal and industrial wastewater treatment plants, *Chemosphere* 88 (2012) 888–894.
- [11] X.L. Zhang, X.J. Luo, S.J. Chen, J.P. Wu, B.X. Mai, Spatial distribution and vertical profile of polybrominated diphenyl ethers, tetrabromobisphenol A, and decabromodiphenylethane in river sediment from an industrialized region of South China, *Environ. Pollut.* 157 (2009) 1917–1923.
- [12] G.B. Qu, J.B. Shi, T. Wang, J.J. Fu, Z.N. Li, P. Wang, T. Ruan, G.B. Jiang, Identification of tetrabromobisphenol A diallyl ether as an emerging neurotoxicant in environmental samples by bioassay-directed fractionation and HPLC-APCI-MS/MS, *Environ. Sci. Technol.* 45 (2011) 5009–5016.

- [13] S.W. Yang, S.R. Wang, F.C. Wu, Z.G. Yan, H.L. Liu, Tetrabromobisphenol A: Tissue distribution in fish, and seasonal variation in water and sediment of Lake Chaohu, China, *Environ. Sci. Pollut. Res.* 19 (2012) 4090–4096.
- [14] K. Jakobsson, K. Thuresson, L. Rylander, A. Sjödin, L. Hagmar, Å. Bergman, Exposure to polybrominated diphenyl ethers and tetrabromobisphenol A among computer technicians, *Chemosphere* 46 (2002) 709–716.
- [15] Z.X. Shi, Y.N. Wu, J.G. Li, Y.F. Zhao, J.F. Feng, Dietary exposure assessment of Chinese adults and nursing infants to tetrabromobisphenol-A and hexabromocyclododecanes: Occurrence measurements in foods and human milk, *Environ. Sci. Technol.* 43 (2009) 4314–4319.
- [16] European Food Safety Authority (EFSA), Scientific opinion on tetrabromobisphenol A (TBBPA) and its derivatives in food. EFSA panel on contaminants in the food chain (CONTAM), *EFSA J.* 9 (2011) 2477–2538.
- [17] H. Viberg, P. Eriksson, Differences in neonatal neurotoxicity of brominated flame retardants, PBDE 99 and TBBPA, in mice, *Toxicology* 289 (2011) 59–65.
- [18] V.K. Gupta, R. Kumar, A. Nayak, T.A. Saleh, M.A. Barakat, Adsorptive removal of dyes from aqueous solution onto carbon nanotubes: A review, *Adv. Colloid Interface Sci.* 193–194 (2013) 24–34.
- [19] Y.H. Zhang, Y.L. Tang, S.Y. Li, S.L. Yu, Sorption and removal of tetrabromobisphenol A from solution by graphene oxide, *Chem. Eng. J.* 222 (2013) 94–100.
- [20] S.B. Wang, C.W. Ng, W.T. Wang, Q. Li, L.Q. Li, A Comparative study on the adsorption of acid and reactive dyes on multiwall carbon nanotubes in single and binary dye systems, *J. Chem. Eng. Data* 57 (2012) 1563–1569.
- [21] X. Yang, C.L. Chen, J.X. Li, G.X. Zhao, X.M. Ren, X.K. Wang, Graphene oxide-iron oxide and reduced graphene oxide-iron oxide hybrid materials for the removal of organic and inorganic pollutants, *RSC Adv.* 2(2012) 8821–8826.
- [22] G.X. Zhao, L. Jiang, Y.D. He, J.X. Li, H.L. Dong, X.K. Wang, W.P. Hu, Sulfonated graphene for persistent aromatic pollutant management, *Adv. Mater.* 23 (2011) 3959–3963.
- [23] S. Agnihotri, J.P.B. Mota, M. Rostam-Abadi, M.J. Rood, Adsorption site analysis of impurity embedded single-walled carbon nanotube bundles, *Carbon* 44 (2006) 2376–2383.
- [24] R. Kumar, M.O. Ansari, M.A. Barakat, Adsorption of brilliant green by surfactant doped polyaniline/MWCNTs composite: Evaluation of the kinetic, thermodynamic, and isotherm, *Ind. Eng. Chem. Res.* 53 (2014) 7167–7175.
- [25] J.L. Hu, Z.L. Tong, Z.H. Hu, G.W. Chen, T.H. Chen, Adsorption of roxarsone from aqueous solution by multi-walled carbon nanotubes, *J. Colloid Interface Sci.* 377 (2012) 355–361.
- [26] J. Hu, D.D. Shao, C.L. Chen, G.D. Sheng, X.M. Ren, X.K. Wang, Removal of 1-naphthylamine from aqueous solution by multiwall carbon nanotubes/iron oxides/cyclodextrin composite, *J. Hazard. Mater.* 185 (2011) 463–471.
- [27] J. Hu, D.D. Shao, C.L. Chen, G.D. Sheng, J.X. Li, X.K. Wang, M. Nagatsu, Plasma-induced grafting of cyclodextrin onto multiwall carbon nanotube/iron oxides for adsorbent application, *J. Phys. Chem. B* 114 (2010) 6779–6785.
- [28] S. Qu, F. Huang, S.N. Yu, G. Chen, J.L. Kong, Magnetic removal of dyes from aqueous solution using multi-walled carbon nanotubes filled with Fe₂O₃ particles, *J. Hazard. Mater.* 160 (2008) 643–647.
- [29] X.W. Zhao, Q. Jia, N.Z. Song, W.H. Zhou, Y.S. Li, Adsorption of Pb(II) from an aqueous solution by titanium dioxide/carbon nanotube nanocomposites: Kinetics, thermodynamics, and isotherms, *J. Chem. Eng. Data* 55 (2010) 4428–4433.
- [30] D.R. Kumar, D. Manoj, J. Santhanalakshmi, Optimization of site specific adsorption of oleylamine capped CuO nanoparticles on MWCNTs for electrochemical determination of guanosine, *Sens. Actuators, B* 188 (2013) 603–612.
- [31] P.H. Chen, C.F. Hsu, D.D.W. Tsai, Y.M. Lu, W.J. Huang, Adsorption of mercury from water by modified multi-walled carbon nanotubes: Adsorption behaviour and interference resistance by coexisting anions, *Environ. Technol.* 35 (2014) 1935–1944.
- [32] J. Hu, Z. Tong, G. Chen, X. Zhan, Z. Hu, Adsorption of roxarsone by iron (hydr)oxide-modified multi-walled carbon nanotubes from aqueous solution and its mechanisms, *Int. J. Environ. Sci. Technol.* 11 (2014) 785–794.
- [33] H.H. Cho, B.A. Smith, J.D. Wnuk, D.H. Fairbrother, W.P. Ball, Influence of surface oxides on the adsorption of naphthalene onto multiwalled carbon nanotubes, *Environ. Sci. Technol.* 42 (2008) 2899–2905.
- [34] Y.H. Zhang, G.C. Liu, S.L. Yu, J. Zhang, Y.L. Tang, P. Li, Y.F. Ren, Kinetics and interfacial thermodynamics of the pH-related sorption of tetrabromobisphenol A onto multiwalled carbon nanotubes, *ACS Appl. Mater. Interfaces* 6 (2014) 20968–20977.
- [35] R.M. Allen-King, P. Grathwohl, W.P. Ball, New modeling paradigms for the sorption of hydrophobic organic chemicals to heterogeneous carbonaceous matter in soils, sediments, and rocks, *Adv. Water Resour.* 25 (2002) 985–1016.
- [36] I.I. Fafous, E.S. Radwan, J.N. Dawoud, Kinetics, equilibrium and thermodynamics of the sorption of tetrabromobisphenol A on multiwalled carbon nanotubes, *Appl. Surf. Sci.* 256 (2010) 7246–7252.
- [37] Y.M. Ren, J. Yang, W.Q. Ma, J. Ma, J. Feng, X.L. Liu, The selective binding character of a molecular imprinted particle for Bisphenol A from water, *Water Res.* 50 (2014) 90–100.
- [38] W. Rudzinski, W. Plazinski, Kinetics of solute adsorption at solid/aqueous interfaces: Searching for the theoretical background of the modified pseudo-first-order kinetic equation, *Langmuir* 24 (2008) 5393–5399.
- [39] J.X. Lin, L. Wang, Comparison between linear and non-linear forms of pseudo-first-order and pseudo-second-order adsorption kinetic models for the removal of methylene blue by activated carbon, *Front. Environ. Sci. Eng. China* 3 (2009) 320–324.

- [40] B. Pan, B.S. Xing, Adsorption kinetics of 17 alpha-ethinyl estradiol and bisphenol A on carbon nanomaterials. I. Several concerns regarding pseudo-first order and pseudo-second order models, *J. Soils Sediment.* 10 (2010) 838–844.
- [41] S. Chowdhury, P. Saha, Adsorption kinetic modeling of safranin onto rice husk biomatrix using pseudo-first- and pseudo-second-order kinetic models: Comparison of linear and non-linear methods, *Clean—Soil Air Water* 39 (2011) 274–282.
- [42] C.R. Lee, H.S. Kim, I.H. Jang, J.H. Im, N.G. Park, Pseudo first-order adsorption kinetics of N719 dye on TiO₂ surface, *ACS Appl. Mater. Interfaces* 3 (2011) 1953–1957.
- [43] Q. Yu, R.Q. Zhang, S.B. Deng, J. Huang, G. Yu, Sorption of perfluorooctane sulfonate and perfluorooctanoate on activated carbons and resin: Kinetic and isotherm study, *Water Res.* 43 (2009) 1150–1158.
- [44] Y. Gao, Y. Li, L. Zhang, H. Huang, J.J. Hu, S.M. Shah, X.G. Su, Adsorption and removal of tetracycline antibiotics from aqueous solution by graphene oxide, *J Colloid Interface Sci.* 368 (2012) 540–546.
- [45] Y. Liu, Is the free energy change of adsorption correctly calculated? *J. Chem. Eng. Data* 54 (2009) 1981–1985.
- [46] J.Y. Chen, W. Chen, D. Zhu, Adsorption of nonionic aromatic compounds to single-walled carbon nanotubes: Effects of aqueous solution chemistry, *Environ. Sci. Technol.* 42 (2008) 7225–7230.
- [47] D.H. Lin, B.S. Xing, Adsorption of phenolic compounds by carbon nanotubes: Role of aromaticity and substitution of hydroxyl groups, *Environ. Sci. Technol.* 42 (2008) 7254–7259.
- [48] W. Chen, L. Duan, L.L. Wang, D.Q. Zhu, Adsorption of hydroxyl- and amino-substituted aromatics to carbon nanotubes, *Environ. Sci. Technol.* 42 (2008) 6862–6868.
- [49] V. Chandra, J. Park, Y. Chun, J.W. Lee, I.C. Hwang, K.S. Kim, Water-dispersible magnetite-reduced graphene oxide composites for arsenic removal, *ACS Nano* 4 (2010) 3979–3986.
- [50] Y.F. Xu, Z.B. Liu, X.L. Zhang, Y. Wang, J.G. Tian, Y. Huang, Y.F. Ma, X.Y. Zhang, Y.S. Chen, A graphene hybrid material covalently functionalized with porphyrin: Synthesis and optical limiting property, *Adv. Mater.* 21 (2009) 1275–1279.